

# On the estimation of the forest fire front position by radiative flux measurement.

M Bergmann, D. Bernardin, S Ramezani, and O Séro-Guillaume  
November 15, 2006

Laboratoire d'Energétique et de Mécanique Théorique et Appliquée,  
UMR 7563 CNRS,  
Avenue de la forêt de Haye, BP 160, 54504 Vandoeuvre-lès-Nancy Cedex, France

## Abstract

This paper presents a method to estimate precisely a forest fire front position which is often undetectable due to the dense smoke released by the fire. Usually, a fire front position is defined by a curve of constant temperature. In this study we propose to use only some measurements of the radiative flux obtained by sensors to estimate the fire front position. The inverse method developed in this paper uses both simplex and conjugate gradient methods. The performance of this method is then demonstrated on a forest fire test case.

## 1. Introduction and Motivation

### 1. Generalities

Let us firstly motivate the study. Some models of forest fire propagation at large scale are reaction diffusion systems, see [1-3] for example, set on the surface of the terrain. They are generally deduced from the balance of energy and the balance of mass for the solid fuel and reduced to a 2D system, and have the following general structures:

Balance of energy:

$$(1 - \Phi)\rho(C_s + H_u C_l) \frac{\partial T}{\partial t} = \nabla \cdot (\lambda \nabla T) + h(T_f - T_g) + (1 - \Phi)\rho \frac{\partial H_u}{\partial t} L_{ev} \delta_{T=T_{ev}} + M_r. \quad (1)$$

and in the zone where pyrolysis occurs, an equation modeling the kinetic of decomposition must be considered:

$$\frac{\partial \rho}{\partial t} = -\rho f(T). \quad (2)$$

In these relations  $T$ ,  $\rho$  and  $\Phi$  represent the temperature, the density of wood, and the porosity of the vegetation,  $C_s$  and  $C_l$  stand for the heat capacity of the dried wood and of water,  $H_u$  is the humidity,  $T_g$  is the temperature of the ambient gas.  $M_r$  is the radiative flux coming from flames,  $\delta_{T=T_{ev}}$  is the characteristic function of the zone of evaporation. This model supposes that the radiative transfer is the main process of heating and corresponds to a case where the totality of the energy received by the fuel is used for evaporating the water during the process of drying. The burning zone is defined by the inequality  $T \geq T_i$ , the fire front being defined by the equality  $T = T_i$ . In fact the propagation of fire in the preceding modeling is a free boundary problem, the evaporation and the burning zones being unknown and parts of the problem. For the sake of simplicity let us assume that there is no humidity,

that is  $H_u = 0$ . Let us enlight the dependency of the problem upon the burning zone, using a V.O.F. formulation [3]. Let  $\chi(\mathbf{x}, t)$  be the characteristic function of the burning zone, i.e. such that  $\chi(\mathbf{x}, t) = 1$  if the point  $x$  lies in the burning zone at time  $t$  and  $\chi(\mathbf{x}, t) = 0$  elsewhere. The characteristic function, considered as a distribution, satisfies the equation, see [4]:

$$\frac{\partial \chi}{\partial t} + \nabla \chi \cdot \mathbf{w} = 0 \quad (3)$$

In relation (3)  $\mathbf{w}$  is the normal velocity of the fire front, it is equal to:

$$\mathbf{w} = - \left. \frac{\frac{\partial T}{\partial t}}{|\nabla T|^2} \nabla T \right|_{T=T_i} . \quad (4)$$

We can consider now a mollifier  $m_h(\mathbf{x})$ , i.e. a function such that  $m_h(\mathbf{x}) > 0$ ,  $\int_{R^2} m_h(\mathbf{x}) d\mathbf{x} = 1$  and the function tends to a Dirac distribution when  $h \rightarrow 0$ . This function can be chosen as smooth as desired, so that the function defined by the convolution:

$$\alpha(\mathbf{x}, t) = (\chi * m_h)(\mathbf{x}, t) = \int_{R^2} \chi(\mathbf{y}, t) m_h(\mathbf{x} - \mathbf{y}) d\mathbf{y} \quad (5)$$

is a regular approximation of the characteristic function  $\chi$ , and can be considered as the ‘‘density’’ of the burning part. Now an approximation of the system of propagation is:

$$(1 - \Phi) \rho C_s \frac{\partial T}{\partial t} = \nabla \cdot (\lambda(\alpha) \nabla T) + M_r(\alpha) - h(T - T_g), \quad (6)$$

$$\frac{\partial \alpha}{\partial t} + \nabla \alpha \cdot \mathbf{w} = 0, \quad (7)$$

$$\frac{\partial \rho}{\partial t} = -\alpha \rho f(T), \quad (8)$$

The velocity  $\mathbf{w}$  is a smooth extension of the normal front velocity given by:

$$\mathbf{w} = - \frac{\frac{\partial T}{\partial t}}{|\nabla T|^2} \nabla T. \quad (9)$$

We will see in the next section the dependency of the radiative flux upon the function  $\alpha$ . The system (6)-(9) is now set on the whole plane  $R^2$ .

## 2. Flame model

Indeed the radiative process is a full 3D process because the flames develop above the vegetation. It is possible to assume a geometric shape of the flame and integrate the radiative transfer equation in order to calculate the heat flux  $M_r$ . However the emissivity and the radiative properties of the flames are not well known. In the context of this paper we will consider only close form of the radiative heat flux as convolution integral between a Green function  $G$  and a rate of emitted heat calculated on the burning zone denoted  $\Omega_f$

$$M_r = \int_{\Omega_f} \varphi(y) G(x - y) dy_1 dy_2, \quad (10)$$

or

$$M_r = \int_{R^2} \alpha(y, t) \varphi(y) G(x - y) dy_1 dy_2. \quad (11)$$

if we use the density of burning part. In expressions (10) or (11) the radiative flux appears clearly as a function of the burning zone. The close form expression (10) can be computed

assuming that the burning zone is thin, the flame is supposed to be at constant known temperature  $T_f$ . Each flame element is supposed to be directed by a unit vector  $\mathbf{F}$  parallel to the velocity of the gas  $\mathbf{V}_f$ , the emitting point is denoted by  $P$  and the receiving point by  $M$ ,  $O$  is the flame foot (cf. Figure 1).

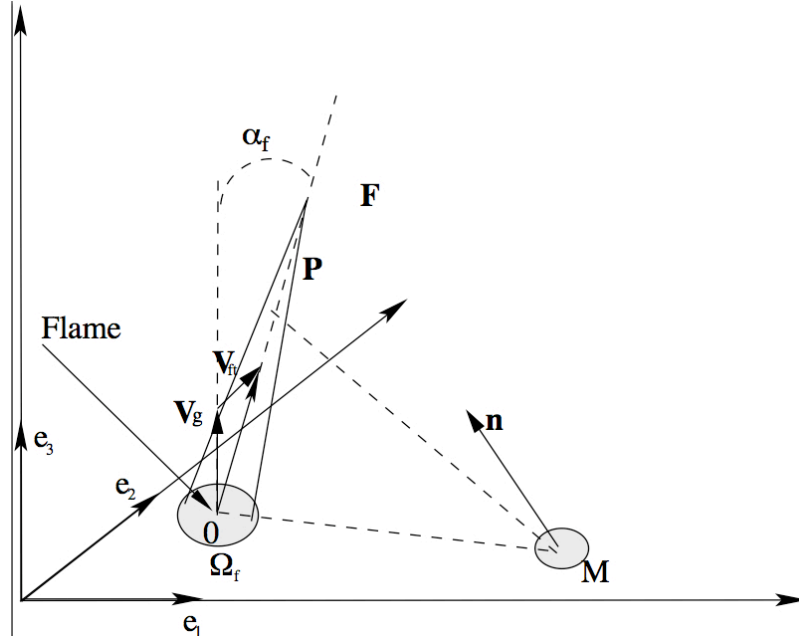


Figure 1. Radiation of the flame.

The global unit vectors of the global co-ordinates system are denoted by  $(\mathbf{e}_1, \mathbf{e}_2, \mathbf{e}_3)$ ,  $\mathbf{e}_3$  being the vertical direction. The vector  $\mathbf{n}$  is the unit normal to the receiving surface of the vegetation at point  $M$ . The angle between  $\mathbf{F}$  and the vertical is denoted by  $\alpha_f = (\mathbf{e}_3, \mathbf{F})$ . The flame elements are supposed to have a length  $l_f$ . One can show cf [4] that the radiative heat flux is given by:

$$M_r = K_f \frac{BT^4}{\pi} \int_{\Omega_f} \frac{(\mathbf{F}(1 - \cos\theta_f) - w(\cos\beta - \cos(\beta + \theta_f))) \cdot \mathbf{n}}{r \sin^2 \beta} dy_1 dy_2, \quad (12)$$

with,  $r$  being the distance between the emitting and the receiving points  $OM = r$ ,  $w = \cos\theta_f$ ,  $K_f$  the absorption coefficient of the flame,  $b = (\mathbf{F}, \mathbf{OM})$ ,  $q = (\mathbf{OM}, \mathbf{PM})$ ,  $\theta_f$  is the maximum value of  $\theta$ ,  $B\sigma = \pi^5/15$ ,  $\sigma$  is the Stefan Boltzmann constant and  $n$  is the reflective index.

The velocity of the gas is the sum of the vertical velocity of the gases and of the wind

$$\mathbf{V}_f = \mathbf{v}_g + \mathbf{V} \quad (13)$$

where  $\mathbf{v}_g = \sqrt{gh_f} \mathbf{e}_3$  is the vertical flame gas velocity, and  $\mathbf{V}$  is the wind velocity.

### 3. Objective of the study

Usually models describing forest fire at large scale like (6)-(9) are compared to measurements obtained in prescribed burnings, see [7], [8]. These types of fires are set on fields of several tenths meters sizes. They usually are instrumented using thermocouples and systems for recovering the fire front position. If the distribution of vegetation is homogeneous and if the

wind is constant the fire front is a straight line for a line ignition, its position can be obtained by the peaks of temperature. If the fire front is no more a straight line, other methods must be elaborated for determining the fire front position. Due to the size of the terrain the use of thermocouples is uneasy and devices using optical remote sensing have been designed [9]. However the determination of the fire front position by optical methods is not so easy because of the size of the field in prescribed burning, of the possibility of smoke. This paper is a methodological paper and the question addressed here is: is it possible to determine the fire line position measuring the radiative flux field? The question of the technology involved in such radiative heat flux measurement has been considered elsewhere [10]. The method developed here is a method of optimal control or inverse method. We consider a discrete version of a functional like  $J = \int_{R^2} |M_r^{cal} - M_r^{mes}|^2 d\omega$  where the calculated radiative flux field

$M_r^{cal}$  is considered as a function of the burning zone via a flame model. In a real experiment the field  $M_r^{mes}$  should be provided by measurements, here it has been calculated by the considered flame model. In some way these values for the measured flux are exact as we don't want here to test or validate the flame model. As mentioned before the use of model (12) is for minimizing the computational cost of this test but here it is a matter of choice. The algorithm for recovering the radiative flux is to minimize  $J$  with respect to the burning zone. For doing that we find an approximate solution to the problem at a first step, the method will be exposed at section 2.1 and then we use a steepest descent algorithm. The point is to find the derivative of the functional with respect to the burning zone. A virtual movement is then imposed to the domain and the derivative is taken along this virtual movement. This is exposed in section 2.2. At paragraph 3 a numerical application is given. We consider a fire front which is an ellipse "perturbated" by a sinus curve. We then apply the preceding strategy of optimization and recover quite sharply the fire front.

## 2. The control algorithms for the determination of the fire front

This section is devoted to the presentation of the optimization algorithms which are used to determine the fire front position starting from some values of the radiative flux measured with sensors. In this study the sensors are uniformly located in space. The number of sensors is  $N_s = N_{s_x} \times N_{s_y}$ , where  $N_{s_x}$  and  $N_{s_y}$  denote the number of rows and columns of sensors. This section is divided into two parts. While the first part is devoted to find an approximate position of the fire front (§ 1), the second part consists in improving this solution to obtain the real fire front position (§ 2).

### 1. Determination of an approximate fire front position

As it was just mentioned above, the objective here is only to find an approximation of the fire front position. After having described the objective function (§ 1), the optimization algorithm based on the Nelder-Mead simplex method is presented (§ 2).

#### 1. Definition of the first objective function

The natural objective is to find for each sensor a (calculated) radiative flux value that is the most closer to the measured radiative flux. Mathematically, the objective function could be written:

$$J = \sum_{i=1}^{N_s} |M_r^{cal}(x_i, \Omega_f) - M_r^{mes}(x_i)|, \quad (14)$$

where  $\Omega_f$  denotes the actual "calculated" burning zone, and the functions  $M_r^{cal}(x_i, \Omega_f)$  take the form:

$$M_r^{cal}(x, \Omega_f) = \int_{\Omega_f} \varphi(y)G(x-y) dy. \quad (15)$$

However, since the radiative flux decreases with distance and tends to zero, the contribution of the  $N_s$  sensors have not the same weight in the objective function (14). Indeed, the sensors located near the fire front are greatly predominant versus the other ones. At this stage it is desirable that all the sensors have the same contribution in the objective function. Thus, to get rid of this problem, the objective function (14) is replaced by the new following objective function:

$$J_1 = \sum_{i=1}^{N_s} \frac{|M_r^{cal}(x_i, \Omega_f) - M_r^{mes}(x_i)|}{\max(M_r^{cal}(x_i, \Omega_f), M_r^{mes}(x_i))}. \quad (16)$$

This objective function represents then the percentage of the error between the measured and the calculated radiative flux where all the sensors have the same weight even if they are located far away the fire front. To simplify future notations, the boundary of the burning zone  $\Omega_f$  is discretized into a vector  $\mathbf{u} = (x_1, y_1, \dots, x_p, y_p)$ ,  $\mathbf{u} \in R^n$ ,  $n = 2p$ . Due to the numerical cut off involves in the radiative flux distribution, it has to be noticed that a sensor has however to be located in the radiative influence zone defined by the parameter  $h_r$  to be activated. In other words, a sensor of index  $i$  at location  $z_i$  is only activated if it is located in a area defined by  $\min_{\mathbf{u}} \text{dist}(z_i, \mathbf{u}) < h_r$ . If not, the sensor is shut down and the objective function takes a value equal to zero. The radiative influence zone around a fire front is schematically represented in figure 3.

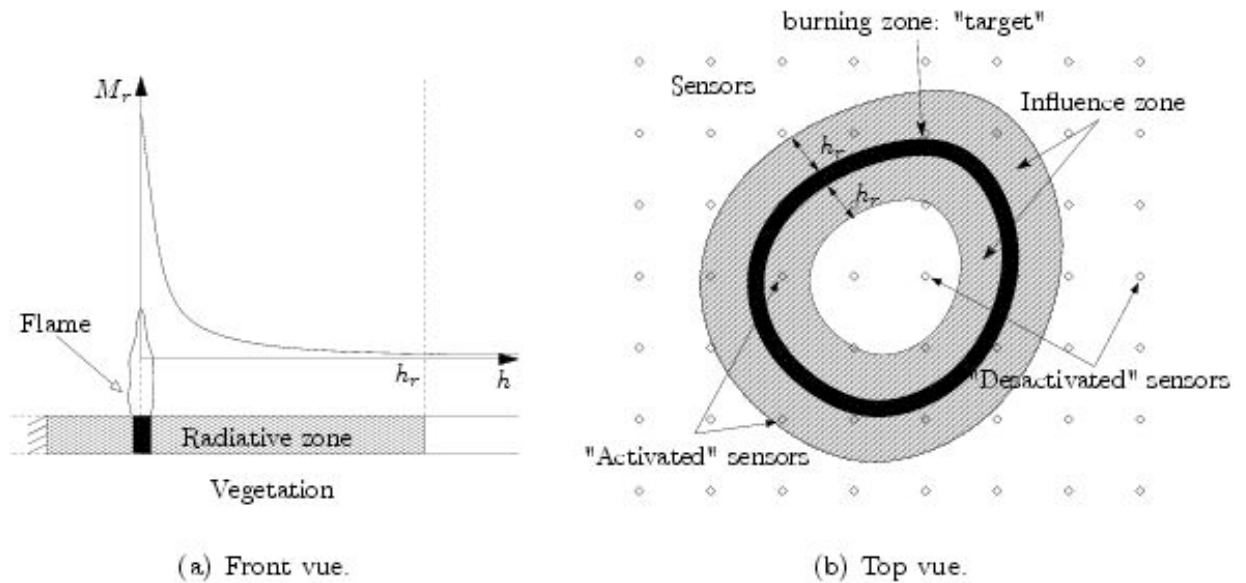
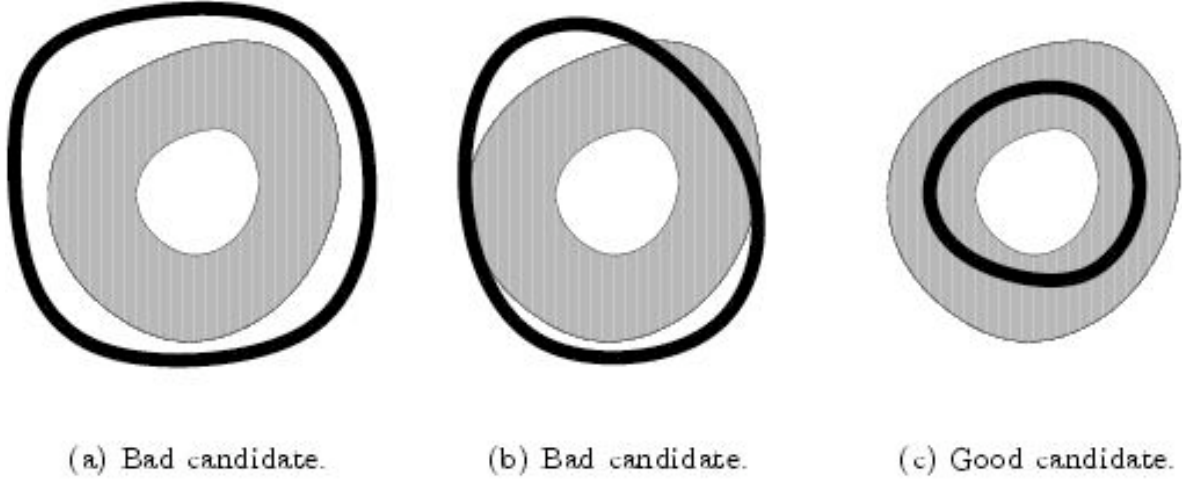


Figure 2. Description of the radiative influence zone.

## 2. Optimisation algorithm: the Nelder Mead simplex method [11 ,12]

Due to the numerical cut off involved in the spatial distribution of the radiative flux, the objective function does not depend on the variations of the sensors positions  $x_i$  when sensors are located far away from the fire front (outside the influence zone). It seems thus to be necessary to start an effective optimisation algorithm based on the gradient of the objective function from a solution which belong to the radiative influence zone as described in figure 4.



**Figure 3. Description of different candidates for fire front that could be obtained by the simplex method. Good candidate belong entirely to the radiative influence zone.**

To get such a solution, a genetic algorithm could be used. Genetic algorithms are often used in many physical disciplinary as geophysics [14], elasticity [15]. But due to the high numerical costs involved using this kind of algorithm we chose to use the Nelder mead simplex method described below.

### **Algorithm 1.** *Nelder Mead simplex method*

Let  $f$  be an objective function such that  $f : R^n \mapsto R$ . A simplex is composed by  $n+1$  different points with coordinates  $\mathbf{u} \in R^n$ . These points could be chosen starting from some knowledge of the objective function, but there are usually chosen arbitrarily.

Initialisation.

Let  $k = 0$ . A initial simplex is arbitrary built. The value of the objective function  $f$  is evaluated at each point  $\mathbf{u}$  of the simplex.

i. Reflection

After having determined  $\mathbf{u}_{max}^k = \operatorname{argmax} f(\mathbf{u}^k)$  we calculate the barycenter  $\bar{\mathbf{u}}^k$  of the  $n$  other points. The point  $\mathbf{u}_{max}^k$  is then reflected versus  $\bar{\mathbf{u}}^k$  to obtain a new point  $\mathbf{u}_{ref}^k$  as follows:

$$\mathbf{u}_{ref}^k = (1 + \alpha)\bar{\mathbf{u}}^k - \alpha\mathbf{u}_{max}^k. \quad (17)$$

The point  $\mathbf{u}_{max}^k$  is then replaced by the point  $\mathbf{u}_{ref}^k$  to get a new simplex.

We often impose at the reflected point  $\mathbf{u}_{ref}^k$  to be the symmetric of the  $\mathbf{u}_{max}^k$  versus the barycenter  $\bar{\mathbf{u}}^k$ , and we thus take  $\alpha = 1$ .

ii. Expansion

If  $f(\mathbf{u}_{ref}^k) \leq f(\mathbf{u}_i^k), \forall i$ , i.e. if the value of the objective function  $f$  evaluated at the reflection point is lesser than the other ones, we try to find a better point in this direction. The point  $\mathbf{u}_{exp}^k$  is then determined by the relation:

$$\mathbf{u}_{exp}^k = \gamma \mathbf{u}_{ref}^k + (1 - \gamma) \bar{\mathbf{u}}^k \quad (18)$$

where  $\gamma$  is an arbitrary parameter that varies generally between 1 and 2 in function of the convexity of the objection function  $f$ .

If  $f(\mathbf{u}_{exp}^k) < f(\mathbf{u}_{ref}^k)$ , the point  $\mathbf{u}_{ref}^k$  is replaced by the point  $\mathbf{u}_{exp}^k$  in the new simplex. If not, the point  $\mathbf{u}_{ref}^k$  is preserved.

iii. Contraction

If  $f(\mathbf{u}_{ref}^k) \geq f(\mathbf{u}_i^k), \forall i$ , i.e. if the value of the objective function  $f$  evaluated at the reflection point is still greater than the other ones, a contraction is realized:

$$\mathbf{u}_{con}^k = \beta \mathbf{u}_{ref}^k + (1 - \beta) \bar{\mathbf{u}}^k. \quad (19)$$

The parameter  $\beta$  is chosen arbitrary and varies generally between 0,2 and 1.

If  $f(\mathbf{u}_{con}^k) < f(\mathbf{u}_{ref}^k)$ , the point  $\mathbf{u}_{ref}^k$  is replaced by the point  $\mathbf{u}_{con}^k$  in the new simplex. If not, a *reduction* is done to adapt the simplex to the topology of the problem under consideration.

iv. Reduction

This stage is only necessary when the three first stages have failed. A homothety is then realized around the point of the simplex  $\mathbf{u}_{min}^k$  corresponding to the minimal value of the objective function  $f$ . The other points of index  $i$  are replaced to give:

$$\mathbf{u}_i^k = \frac{\mathbf{u}_i^k + \mathbf{u}_{min}^k}{2}. \quad (20)$$

If  $f(\mathbf{u}_{ref}^k) > f(\mathbf{u}_{max}^k)$  a reduction is applied to the initial simplex: steps (ii), (iii) and (iv) are then ignored.

If  $f(\mathbf{u}_{ref}^k) < f(\mathbf{u}_{max}^k)$  a reduction is applied on the reflected simplex: steps (iii) and (iv) are then ignored.

This algorithm could be stopped when a fire front which belong entirely to the radiative influence zone is obtained (see for example figure 4(c)). But due to its rapidity, it is only stopped when the decrease of the objective function (in fact the average of the function evaluated on the whole simplex) between two successive iterations is smaller than a given parameters  $\varepsilon$ .

The choice of the values of the parameters  $\alpha$  and  $\beta$  is very important in the resolution process. Indeed, they have a direct influence on the simplex topology. In order to reduce the risks of a convergence towards a solution that does not correspond to the minimum, a judicious choice is to take values around 1. In this case the simplex topology is almost not modified and a bad convergence due the brutal contracting could be avoided.

The optimization algorithms based on simplex method are *a priori* effective, at least on some configurations: however there is no mathematical proof of convergence towards the minimum of a function  $f : R^n \mapsto R$  for  $n \geq 2$  (see [13] for more details).

## 2. Determination of a precise solution for the fire front

We can consider now that we have obtained a fire front which belongs to the radiative influence zone (as for example the one of figure 3(c)). Starting from this solution we can improve the result using a more precise optimization algorithm based on the gradient of the objective function. The next paragraph is then devoted to derive analytically the gradient of the objective function.

### 1. Definition of the new objective function and its gradient

Due to the absolute value involved in the objective function (16), the gradient of the objective function is not differentiable. We will thus introduce the new objective function:

$$J_2 = \sum_{i=1}^{N_s} \frac{(M_r^{cal}(x_i, \Omega_f) - M_r^{mes}(x_i))^2}{(M_r^{mes}(x_i))^2}. \quad (21)$$

To evaluate the gradient of the objective function we can consider an infinitesimal virtual movement of the fire front defined by a virtual time  $\varepsilon$  and a virtual velocity  $\boldsymbol{\tau}$ :

$$\mathbf{u} \rightarrow \mathbf{u} + \varepsilon \boldsymbol{\tau}(\mathbf{u}). \quad (22)$$

Using this movement the domain  $\Omega_f$  is transformed in a new burning area  $\overline{\Omega}_f(\varepsilon)$  and the new objective functional writes:

$$\overline{J}_2 = \sum_{i=1}^{N_s} \frac{(M_r^{cal}(x_i, \overline{\Omega}_f) - M_r^{mes}(x_i))^2}{(M_r^{mes}(x_i))^2}. \quad (23)$$

The differential  $\frac{\partial J_2}{\partial \Omega_f}$  is then defined by:

$$\frac{\partial J_2}{\partial \Omega_f} = \left. \frac{\partial \overline{J}_2}{\partial \varepsilon} \right|_{\varepsilon=0}. \quad (24)$$

Considering

$$\overline{M}_r^{cal}(\mathbf{x}, \varepsilon) = M_r^{cal}(\mathbf{x}, \overline{\Omega}_f(\varepsilon)), \quad (25)$$

the differential of the objective function can be written:

$$\frac{\partial J_2}{\partial \Omega_f} = 2 \sum_{i=1}^{N_s} \frac{(M_r^{cal}(x_i, \Omega_f) - M_r^{mes}(x_i))}{(M_r^{mes}(x_i))^2} \cdot \left. \frac{\partial \overline{M}_r^{cal}(x_i, \varepsilon)}{\partial \varepsilon} \right|_{\varepsilon=0}. \quad (26)$$

Using the Reynolds theorem for derivation of integral depending on time we obtain the line integral,  $\mathbf{n}$  being the outward unit normal to the fire front:

$$\left. \frac{\partial \overline{M}_r^{cal}(x_i, \varepsilon)}{\partial \varepsilon} \right|_{\varepsilon=0} = \int_{\partial \Omega_f} \varphi(y) G(x_i - y) \boldsymbol{\tau} \cdot \mathbf{n} ds_y. \quad (27)$$

Using equations (26) and (27) one can obtain:

$$\frac{\partial J_2}{\partial \Omega_f} = 2 \sum_{i=1}^{N_s} \frac{(M_r^{cal}(x_i, \Omega_f) - M_r^{mes}(x_i))}{(M_r^{mes}(x_i))^2} \int_{\partial \Omega_f} \varphi(y) G(x_i - y) \boldsymbol{\tau} \cdot \mathbf{n} ds_y, \quad (28)$$

such that the steepest descent direction is defined by:

$$\boldsymbol{\tau} \Big|_{\partial\Omega_f} = -2 \sum_{i=1}^{N_s} \frac{(M_r^{cal}(x_i, \Omega_f) - M_r^{mes}(x_i))}{(M_r^{mes}(x_i))^2} \int_{\partial\Omega_f} \varphi(y) G(x_i - y) \mathbf{n}(y) ds_y. \quad (29)$$

Finally, if the boundary of the burning zone  $\partial\Omega_f$  is discretized into a vector  $\mathbf{u} \in R^n$ , the gradient of the objective function with respect to the control parameters  $\mathbf{u}$  is:

$$\nabla_{\mathbf{u}} J_2 = -2 \sum_{u_j \in \partial\Omega_f} \sum_{i=1}^{N_s} \frac{(M_r^{cal}(x_i, \mathbf{u}) - M_r^{mes}(x_i))}{(M_r^{mes}(x_i))^2} \varphi(u_j) G(x_i - u_j) \boldsymbol{\tau}(u_j) \mathbf{n}(u_j). \quad (30)$$

## 2. Optimisation algorithm: the conjugate gradient method

for sake of completeness we recall the general resolution process for non linear conjugate gradient methods that we used, in algorithm 2. More details could be found in [16].

### Algorithm 2. Conjugate gradient method

Given an initial set of control parameters  $\mathbf{u}_0$ , evaluate  $f_0 = f(\mathbf{u}_0)$  and  $\nabla_{\mathbf{u}} f_0 = \nabla_{\mathbf{u}} f(\mathbf{u}_0)$ . The algorithm is initialized by a simple gradient step, i.e.  $\mathbf{d}_0 = -\nabla_{\mathbf{u}} f_0$ , where the vector  $\mathbf{d}$  denotes the direction of descent.

While a stopping criterium is not satisfied:

- i. Determination of a step  $\alpha_k$  using one favorite line search method (Wolfe, Armijo, etc). Calcul of a new iterate  $\mathbf{u}_{k+1} = \mathbf{u}_k + \alpha_k \mathbf{d}_k$  ;
- ii. Evaluation of a new gradient  $\nabla_{\mathbf{u}} f_{k+1}$  ;
- iii. Calcul of a parameters  $\beta_{k+1}$  using one favorite conjugate gradient method (Fletcher-Reeves, Polack-Ribière or Hestenes-Stiefel);
- iv. Construction of a new direction of descent  $\mathbf{d}_{k+1} = -\nabla_{\mathbf{u}} f_{k+1} + \beta_{k+1} \mathbf{d}_k$
- v. Incrementation :  $k = k+1$ ;

Usually, this process is stopped when  $\|\nabla_{\mathbf{u}} f\|_2 < \varepsilon$ , where  $\varepsilon$  is an arbitrary small parameter.

In this study we have chosen the Polack-Ribière method to evaluate the value of the parameter  $\beta_{k+1}$  of step (iii):

$$\beta_{k+1} = \frac{\nabla_{\mathbf{u}} f_{k+1}^T (\nabla_{\mathbf{u}} f_{k+1} - \nabla_{\mathbf{u}} f_k)}{\nabla_{\mathbf{u}} f_k^T \nabla_{\mathbf{u}} f_k}. \quad (31)$$

The determination of the step  $\alpha$  involved in step (i) of the algorithm 2 is presented by algorithm 32.

### Algorithm 3. Backtracking Armijo method

Initialisations: choice of a step  $\alpha_k^1 > 0$  and choice of a parameter  $\tau \in ]0, 1[$ .  $i = 1$ .

- i. If the step  $\alpha_k^i$  satisfies the Armijo relation

$$f(\mathbf{u}_k + \alpha_k^i \mathbf{d}_k) \leq f(\mathbf{u}_k) + \omega_1 \alpha_k^i \langle \nabla f_k, \mathbf{d}_k \rangle, \quad (32)$$

it is accepted and the process is stopped. If not:

- ii. We chose  $\alpha_k^{i+1} \in [\tau \alpha_k^i, (1 - \tau) \alpha_k^i]$ ,

- iii. incrementation  $i = i + 1$  and  $\alpha_k = \alpha_k^i$ . Return to step (i).

The value of the parameter  $\tau$  is chosen arbitrary. Usually, it is taken to be equal to  $10^{-2}$ . The step (ii) of the preceding algorithm is often done by interpolation. The step obtained using this algorithm is called Armijo step. Note that sometimes during the optimisation process some steps  $\alpha$  that does not satisfy relation (32) are accepted, that mimics simulated annealing process [14,16].

#### 4. Some computational application

It is experimentally shown (see [17] for example) that a fire ignited by a point in a uniform forest under the action of wind or slope can develop as a curve like an ellipsis with the great axis aligned with wind or slope direction. The experimental (measured) fire front position which has to be recovered using the above optimization algorithms is thus chosen to be an ellipsis. The great axis of the ellipsis is arbitrary chosen to be equal to  $130m$  while the other one is equal to  $100m$ . Moreover, this fire front position is pertubated using a sinus line. So that the equation for the new boundary in polar co-ordinate is  $\rho(\theta) = r(\theta) + a \sin(2\pi nr\theta/2\pi r) = r(\theta) + a \sin(n\theta)$ . The fire front position under consideration, as well as the corresponding radiative influence zone introduced in section 1 are represented in figure 4.

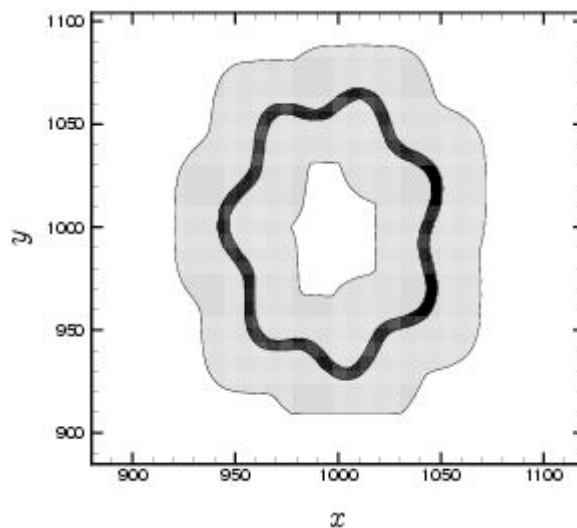


Figure 4. "Target" fire line (black area) and radiative influence zone (gray area).

The fire is supposed to be contained in the close line of figure 4. The measured fluxes are then computed using the last relation for  $\rho(\theta)$  and the following parameters for the flame (table 1):

$K_f = 0.2 m^{-1}$	$T_f = 1200 K$
$l_f = 2 m$	

Table 1. Parameters values of the flame model.

As it was already mentioned, the aim of this study is to recover the fire line using control algorithms. Results of the simplex method and of the conjugate gradient method are presented in section 3.1 and 3.2 respectively. The influence of the number of sensors onto the effectiveness of the estimation of the fire front position is also presented in section 3 of this

paragraph.

### 1. Results of the simplex optimization process

The simplex optimization process described by algorithm1 is carried out. The evolution of the objective function value versus the number of simplex optimization iterations is presented in Figure 5. It is noticeable that after 400 iterations the value of the objective function passes from an initial value equal to 0,67 to a value equal to 0,43. Moreover one can see that after approximately 140 iterations the simplex undergoes an effective reduction step, the value of the objective function passing from a value equal to 0,57 to a value equal to 0,51. Once the simplex optimization process has converged, or more precisely after 400 iterations, the fire front obtained is represented in figure 6. This line is entirely contained in the radiative influence zone also presented in the same figure. In the following, this fire line is taken as the initial condition in a conjugate gradient optimization process.

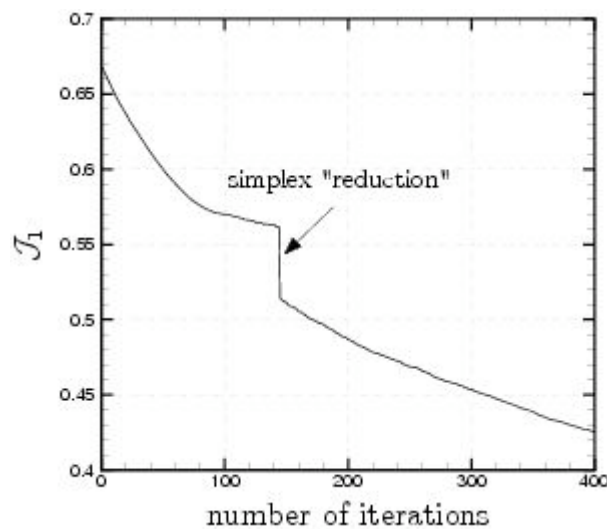


Figure 5. Evolution of the objective function  $J_1$  versus the number of iterations.

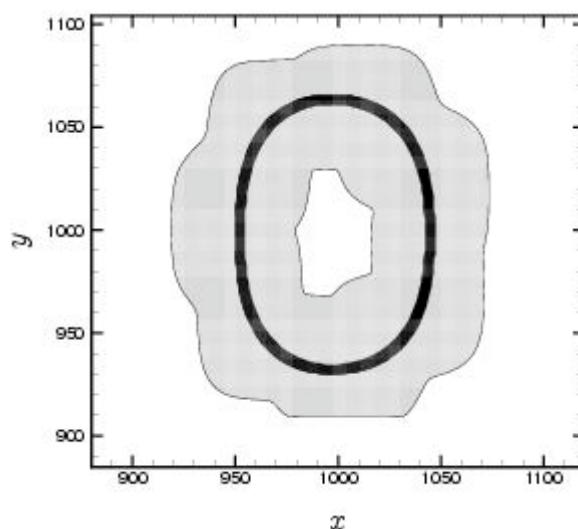


Figure 6. Fire line (black area) obtained by the simplex method. The initial radiative influence zone (gray area) is also presented.

## 2. Results of the conjugate gradient optimization process

The conjugate gradient optimization process described by algorithm 2 is carried out. It is coupled with the backtracking Armijo line search presented by algorithm 3. As it is mentioned above, the fire line obtained using the simplex method is used as initial condition. It is noticeable that the initial value of the objective function does not correspond to that obtained after 400 iterations of the simplex method. Indeed, we have chosen an other objective function in this section (see § 2). As it is shown in figure 8, after only 100 iterations of the conjugate gradient process (500 iterations with the simplex process), the objective function passes from a value equal to 40 to a value equal to 0,01. As it can be shown in figure 7, some peaks corresponding to simulated annealing are visible. The fire line obtained at the end of the conjugate gradient optimization process is presented in figure 8. This line looks like the target presented in figure 4.

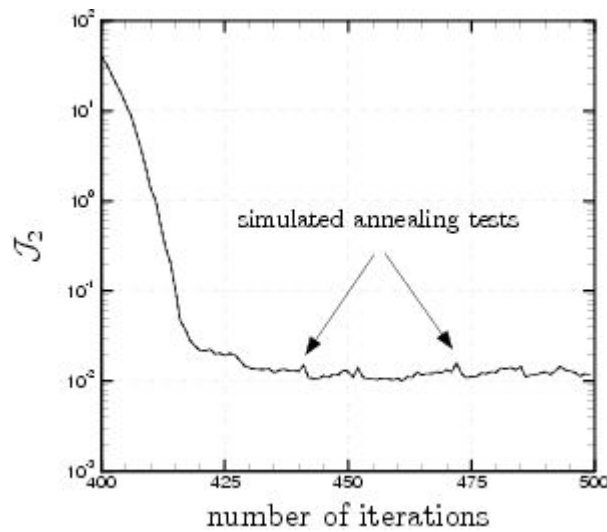


Figure 7. Evolution of the objective function  $J_2$  versus the number of iterations.

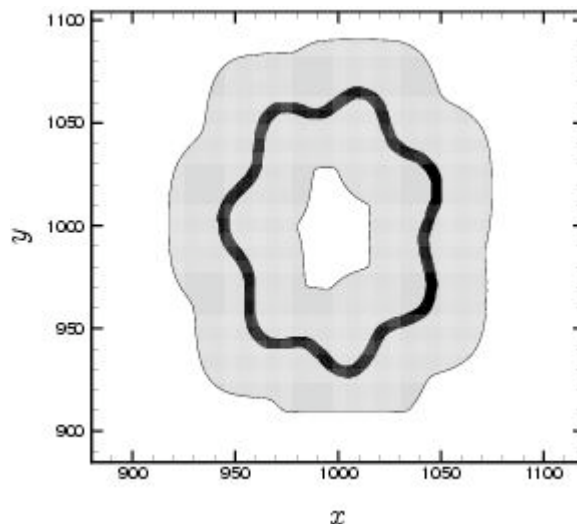
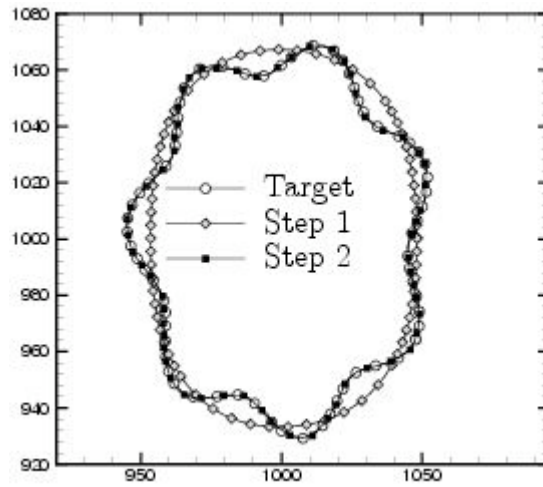


Figure 8. Fire line (black area) obtained by the conjugate gradient method. The initial radiative influence zone (gray area) is also presented.

The results of the simplex (steps 1) and the conjugate gradient (step 2) optimization process are synthesized in figure 9. While the fire line obtained by the simplex method corresponds

approximately to the unperturbed target fire front *i.e.* the ellipse, the fire line obtained by the conjugate gradient method recovers the perturbed target fire front.



**Figure 9.** Comparison of the real fire line, the fire line obtained after the simplex process and the fire line obtained after the conjugate gradient process.

### 3. Influence of the numbers of sensors

This section is devoted to test the influence of the number of sensors onto the effectiveness of the estimation of the fire front position. To make such a test, we represent the evolution of the converged value of the second objective function, *i.e.*  $J_2$ , versus the number of sensors in figure 11. As one can show in this figure, the function  $J_2$  reaches a minimum for a value of the number of sensors in both  $x$  and  $y$  directions equal to 100. Due to the threshold reached by the function  $J_2$  as from  $N_x = N_y = 100$  (see figure 10) it is not necessary to take more sensors. In other words, since the fire front chosen in this study measured approximately  $200m \times 200m$ , the optimal distance between two sensors must be equal to  $2m$ . The number of sensors is then very high (10,000) to estimate quasi-perfectly the whole fire front position (see figure 9). However, as this study is really interesting to calibrate some fire propagation models, it is not necessary to estimate whole fire front position but only some part of it as it is done usually in some experiments.

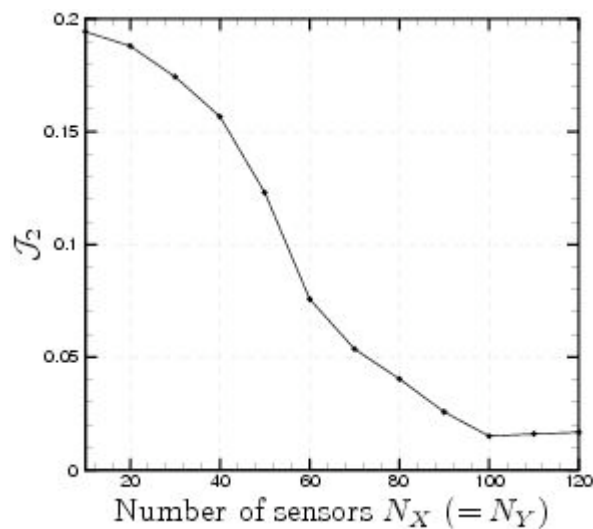


**Figure 10. Evolution of the function  $J_2$  versus the number of sensor.**

Indeed, we have to calibrate the propagation model onto an experimental fire line with length equal to 20m which propagates during 10m approximatively. Thus, only 50 sensors seem to be necessary.

## 5. Conclusion

This study is a preliminary work for the definition of a metrology of prescribed fire used for the validation of propagation model of forest fires. Within the context of a flame model we have shown how the fire front can be reconstructed, and then proposed an inverse method to estimate the forest fire front position from some radiative flux measurements obtained by “radiative sensors”. This inverse method involves two sages: the first one with the objective defined by (16) which has been minimized by simplex algorithm. This choice: functional defined by (16) and simplex algorithm has revealed to be the fastest algorithm for setting “acceptable fire front”. The second step is a refinement of the initial step the functional is defined by (21) and then a conjugate gradient methods is used for improving the result of the first minimization. This method has been tested on an arbitrary forest fire. The solution obtained by this inverse method converges towards the desired fire front with a relatively low computational cost. In a real fire there is uncertainty on the flame model, i.e. the radiative parameters of the flame and of the vegetation are not exactly known. The method presented here should be extended to Bayesian estimation and solving the complete radiative transfer equation.

## References

- [1] Weber R.O., 1991, Toward a comprehensive wildfire spread model, *Int J. Wildland Fire*, 1, 245-248
- [2] Margerit J, Séro-Guillaume O., 2002 Modelling of Forest Fires Propagation Part II, Reduction to Two Dimensional Models and Simulation of Propagation *Int. J. Heat and Mass Transfer*.
- [3] Ferragut L., Asensio M.I., Monedero S., Modelling Radiation and Moisture content in fire spread, *Commun. Numer. Met. Engng*, 2006, in press (available on line).
- [4] Hirt CW and Nichols BD 1981 Volume of Fluid (VOF) method for the Dynamics of Free Boundaries *Journal of Computational Physics* 201-225.
- [5] Bergmann M., Séro-Guillaume O., Ramezani S., Note on the determination of the ignition in forest fire propagation using a control algorithm, *Commun. Numer. Met. Engng*, 2007, in press (available on line).
- [6] Estrada R. and Kanwal R.P. 1980 Applications of Distributional Derivatives to Wave Propagation *J. Inst. Maths Applies* 26, 39-63
- [7] D.X. Viegas, P.M. Palheiro, L.P. Pita, L.M. Ribeiro, M.G. Cruz, A. Ollero, B. Arrue, and M. Dios Ramiro 2006, Analysis of fire behaviour in Mediterranean shrubs: The Gestosa fire experiments (Portugal). ABSTRACT. *Forest Ecology and Management*, volume 234, Supplement 1, 15 November 2006, page S101.
- [8] P.A. Santoni, A. Simeoni, J.L. Rossi, F. Bosseur, F. Morandini, X. Silvani, J.H. Balbi, D. Cancellieri and L. Rossi 2006 Instrumentation of wildland fire : Characterisation of a fire spreading through a Mediterranean shrub. *Fire Safety Journal*, volume 41, Issue 3, p 171-184.
- [9] E. Pastor, A. Águeda, J. Andrade-Cetto, M. Muñoz, Y. Pérez and E. Planas, 2006,

Computing the rate of spread of linear flame fronts by thermal image processing. *Fire Safety Journal*, volume 41, p 569-579.

[10] K. Chetehouna, O. Séro-Guillaume, A. Degiovanni: "Measurement of radiative absorption coefficient for a vegetal medium", *Measurement Science and Technology*, vol. 15, N43-N46, 2004.

[11] Nelder JA and Mead R 1965 *Comput. J.* 308-313

[12] Nocedal J and Wright SJ 1999 *Numerical Optimization* (Springer series in operations research)

[13] Lagarias JC, Reeds JA, Wright MH and Wright PE 1998 Convergence properties of the Nelder-Mead simplex method in low dimensions *Siam J. Optim.* 112-147

[14] Ingber L and Rosen B 1992 Genetic algorithms and simulated annealing: a comparison *Math. Comput. Modelling* 87-100

[15] Chiroiu C, Munteanu L, Chiroiu V, Delsanto PP and Scalerandi M 2000 A genetic algorithm for determination of the elastic constants of a monoclinic crystal *Inverse Problems* (1) 121-132

[16] Sambridge M 1998 Exploring multidimensional landscapes without a map *Inverse Problems* (3) 427-440

[17] Peet GB 1967 The shape of mild fires in Jarrah forest *Aus. Forestry* 121-127

